

Electronic Supplementary Information (ESI)

Pseudo-Multicolor Carbon Dots Emission and the Dilution-Induced
Reversible Fluorescence Shift

*Yu-Cheng Chen, Cheng-Yung Nien, Karunya Albert, Cheng-Che Wen, You-Zung
Hsieh and Hsin-Yun Hsu**

Department of Applied Chemistry and Institute of Molecular Science,
National Chiao-Tung University, No.1001 Ta-Hsueh Road, Hsinchu 30010, Taiwan.

METHODS

Synthesis of CDs

Deionized (DI) water (15 mL for each reaction) was first added in the stainless steel autoclave (Hydrion Scientific Instruments, Baltimore, MD) and the required amount of solid L-Arginine (#A8094, Sigma) was employed to achieve expected concentration (1, 2, and 3 M). Under high temperature/pressure in the reactor, the input arginine powders can totally be dissolved after this hydrothermal heating procedure at 180°C for 3, 6, 9, and 12 h, followed by cooling to room temperature. The suspensions were dialyzed for 6 h in DI water using a membrane (MWCO = Nominal 1000, Orange Scientific, Belgium) to obtain light yellow–brown, purified CDs.

Characterization of CDs

The purified CD suspensions were analyzed by atomic force microscopy (AFM, Veeco DiInnova, Veeco Instruments Inc., Plainview, NY). The IR spectra were measured using Fourier-transform infrared spectrometer (Varian 3100 FTIR, Varian, Palo Alto, CA). Raman spectra were obtained using a Raman microscope (DXR™, ThermoFisher Scientific Inc., Waltham, MA). The high-resolution transmission electron microscopy (ARM200F-HRTEM, JEOL, Japan), in-situ multi-functional X-ray diffractometer (In-situ XRD, APEX DUO single crystal diffraction, Bruker, Taiwan) and X-ray photoelectron spectroscopy (XPS, Microlab 350, VG Scientific, UK) were performed in the core facility at the National Chiao-Tung University, Taiwan. The fluorescence spectra (200–900 nm) were measured using a fluorescence spectrophotometer (F700, Hitachi, Japan). The near-IR fluorescence spectra were obtained using a system built in-house. In brief, a 488-nm laser (Coherent Inc., Germany) was focused on the CD samples with an objective lens (N.A. 0.45, LMM-40X-UVV, Thorlab, USA). The signals were processed using a spectrograph (SR-303i-A, ANDOR, Ireland) equipped with a cooled CCD (DV491A-1.7, ANDOR, Ireland).

The quantum yield of the fluorescent CDs was calculated using to the following Equation (1):

$$\varphi = \varphi_R \frac{I \text{ } OD_R n^2}{I_R \text{ } OD n_R^2}$$

where φ is the quantum yield, I is the measured integrated emission intensity, OD is the optical density, and n is the refractive index. The subscript R represents a known fluorophore reference (*e.g.* quinine sulfate: $\varphi = 0.54$ in 0.1 M H₂SO₄). To examine potential photo-bleaching effects, the CD suspensions were subjected to continuous exposure to a fluorescent lamp (18 W, 380–760 nm) for over 1 month, and the fluorescence intensity was measured using a fluorescence microplate reader (FLX 800, BioTek, Winooski, VT). The pH stability of the CDs was examined by preparation of CDs in PBS buffer under a pH gradient of 3–11, and the fluorescence was measured.

Cytotoxicity assay and fluorescence imaging in vitro and in vivo

The cytotoxicity of the CDs was evaluated by incubating CDs (1 mg/mL) with HCT 116 cells overnight. The collected cell suspensions were reacted with 50 μ L of MTT solution (5 mg/mL) for 1 h, and the absorbance at 570 nm was measured. Maintenance of zebrafish (*Danio rerio*) was according to the protocols from Taiwan Zebrafish Core Facility. The CD-fed HCT116 cells and young zebrafish (4-day post fertilization) were imaged using a confocal laser scanning microscope (SP5, Leica, Germany). All experiments were carried out following approval from the Institutional Animal Care and Use Committee of NCTU.

Table S1. Summary of the quantum yield of the synthesized CDs.

(180°C, 1 M, 9 h)	Quantum yield (%)
glutamine	17.8
asparagine	25.18
phenylalanine	3.96
tryptophan	13.75
glutamic acid	3.26
aspartic acid	5.83
arginine	32.6
histidine	4.51
glycine	20.09
serine	7.32

Table S2. Comparison of the quantum yield of synthesized CDs in various solvents and that of pure water.

	Quantum yield ratio (%)			
	H₂O/ H₂O	MeOH/ H₂O	DMSO/ H₂O	DMF/ H₂O
CD _{1,3}	1	0.62	*	*
CD _{1,6}	1	0.68	0.39	0.06
CD _{1,9}	1	0.78	0.58	0.34
CD _{1,12}	1	0.86	0.64	0.30
CD _{2,9}	1	0.81	0.65	0.41
CD _{3,9}	1	0.98	0.50	0.44

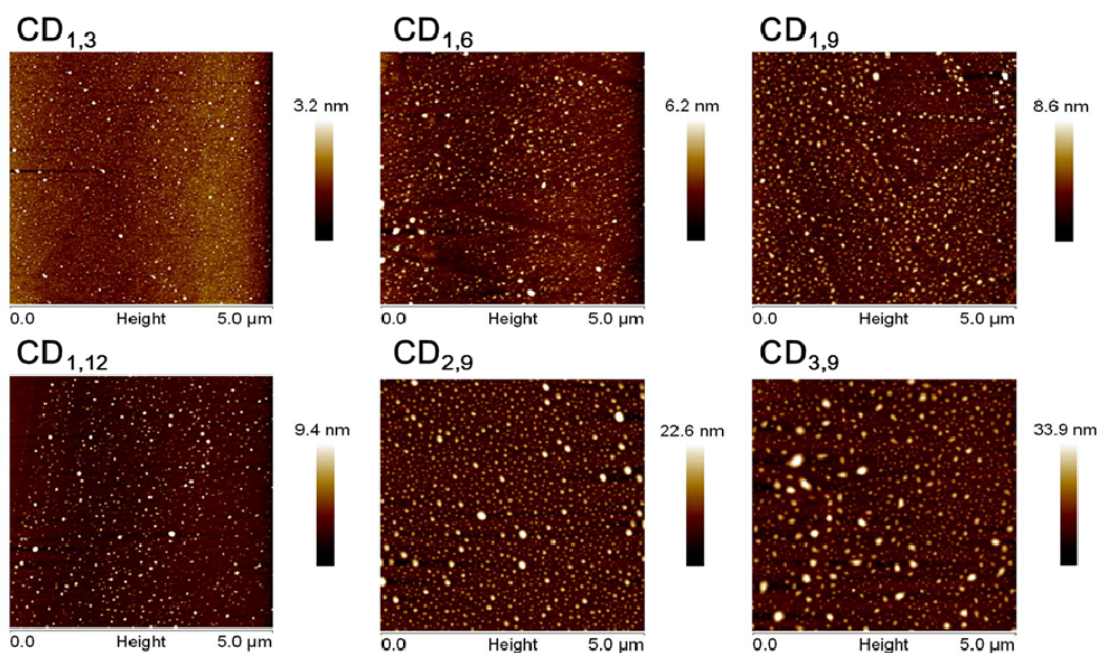


Figure S1 Carbon dots synthesized at specified concentrations (Molarity, M) and times (hours, h) are abbreviated as $CD_{\text{concentration,time}}$. Atomic force microscopy (AFM) measurement shows the average diameter of the CDs was $2.1 \text{ nm} \pm 0.8 \text{ nm}$ ($CD_{1,3}$), $3.2 \text{ nm} \pm 1.3 \text{ nm}$ ($CD_{1,6}$), $4.7 \text{ nm} \pm 1.2 \text{ nm}$ ($CD_{1,9}$), $5.6 \text{ nm} \pm 1.3 \text{ nm}$ ($CD_{1,12}$), $8.7 \text{ nm} \pm 3.7 \text{ nm}$ ($CD_{2,9}$) and $10.9 \text{ nm} \pm 3.4 \text{ nm}$ ($CD_{3,9}$). The spherical CDs were well dispersed, and the average size of the CDs increased as reaction time and precursor concentration increased.

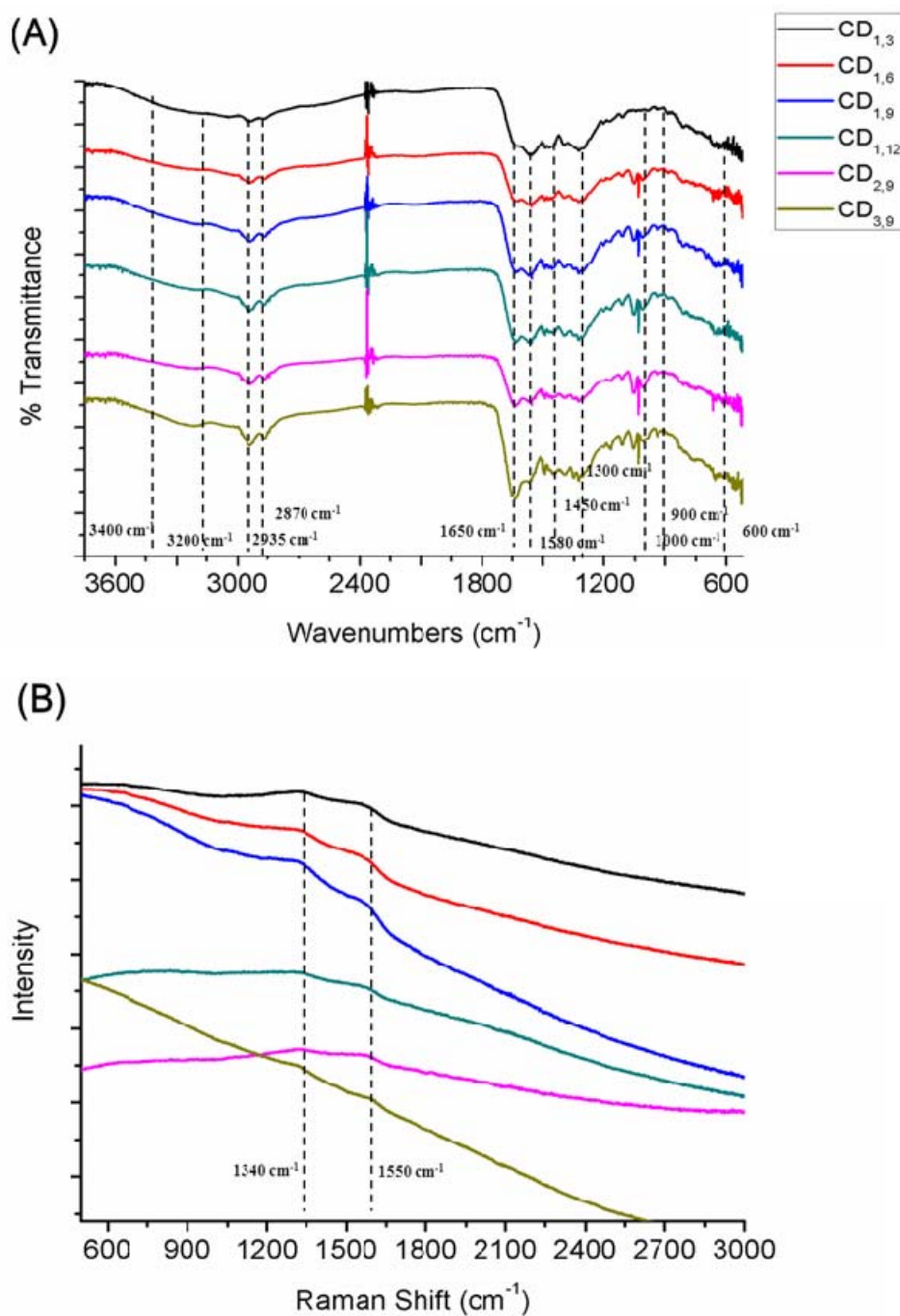


Figure S2 Chemical characteristics of different CDs (A) FTIR spectrum, (B) Raman spectrum. (A) The FT-IR peak of amide I stretching (1650 cm^{-1}), amide II (1580 cm^{-1}), amide III (1450 cm^{-1}) C-N stretching, and C-O vibration peaks ($1000\text{--}1300 \text{ cm}^{-1}$) were enhanced in the CDs synthesized using a high precursor concentration and a prolonged reaction time. The broad peak at $3200\text{--}3400 \text{ cm}^{-1}$ represents hydroxyl O-H stretching. A high passivation level leads to increased nitrogen and oxygen

incorporation; A similar trend can also be observed in the split bands at 2870 cm^{-1} and 2935 cm^{-1} , which resulted from sp^3 C-H stretching, and in the broad band at $600\text{--}900\text{ cm}^{-1}$, which was typically due to out-of-plane bending in graphitic domains. (B) Two characteristic bands, D and G, in Raman spectra of CDs were found in all samples. The D band at 1340 cm^{-1} corresponds to the vibration of dangling bonds of carbon atoms in a disordered graphitic sp^2 network, and the band near 1550 cm^{-1} is associated with the $\text{e}_{2\text{g}}$ in-plane stretching vibration mode. However, the Raman spectra of these CDs appeared featureless at their characteristic D and G peaks with increasing reaction time and concentration; this is probably due to the enhanced intrinsic photoluminescence background of CDs during synthesis.

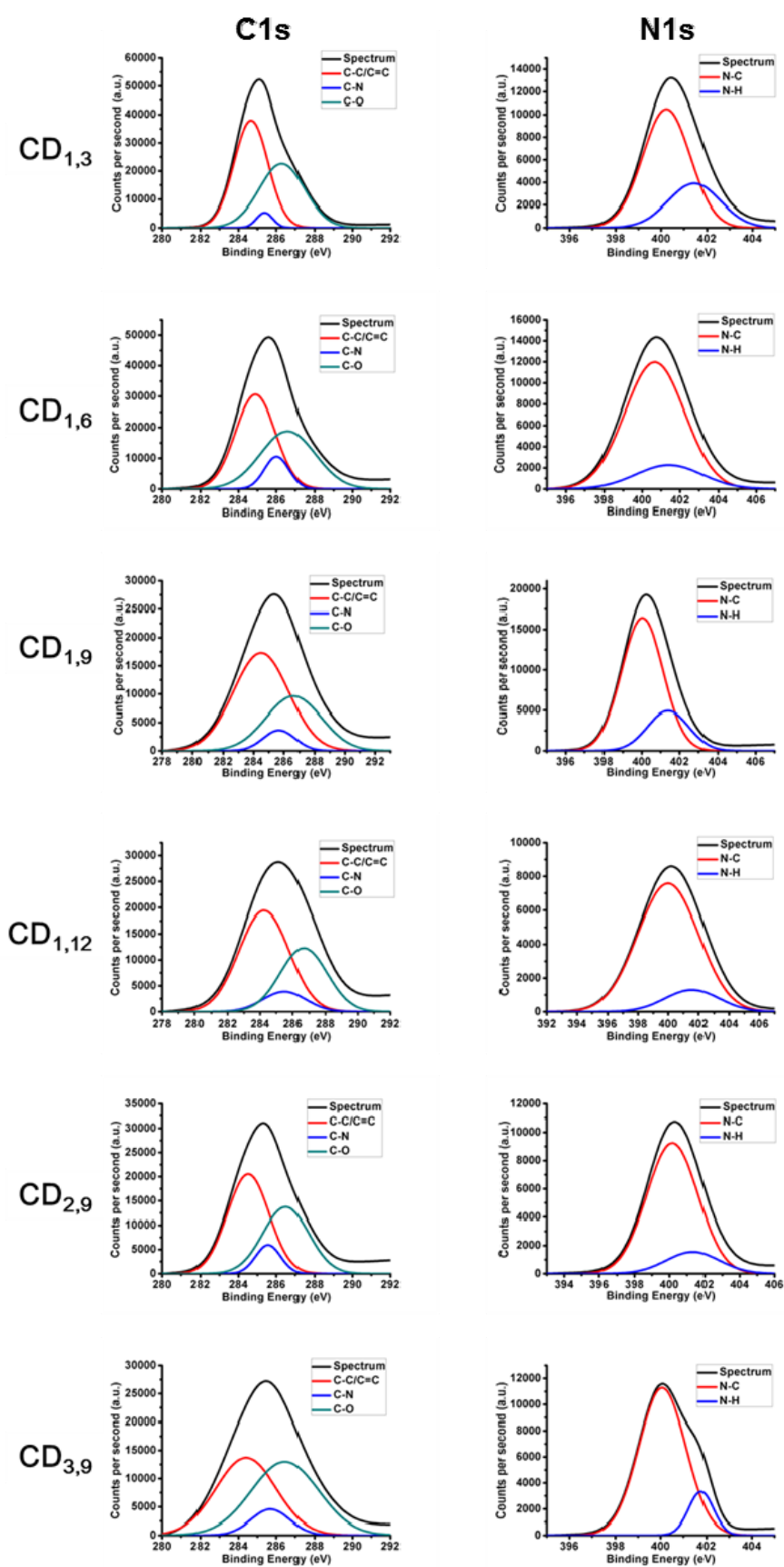


Figure S3. Deconvoluted high-resolution C1s and N1s XPS spectra to reveal the chemical characteristics of synthesized CDs.

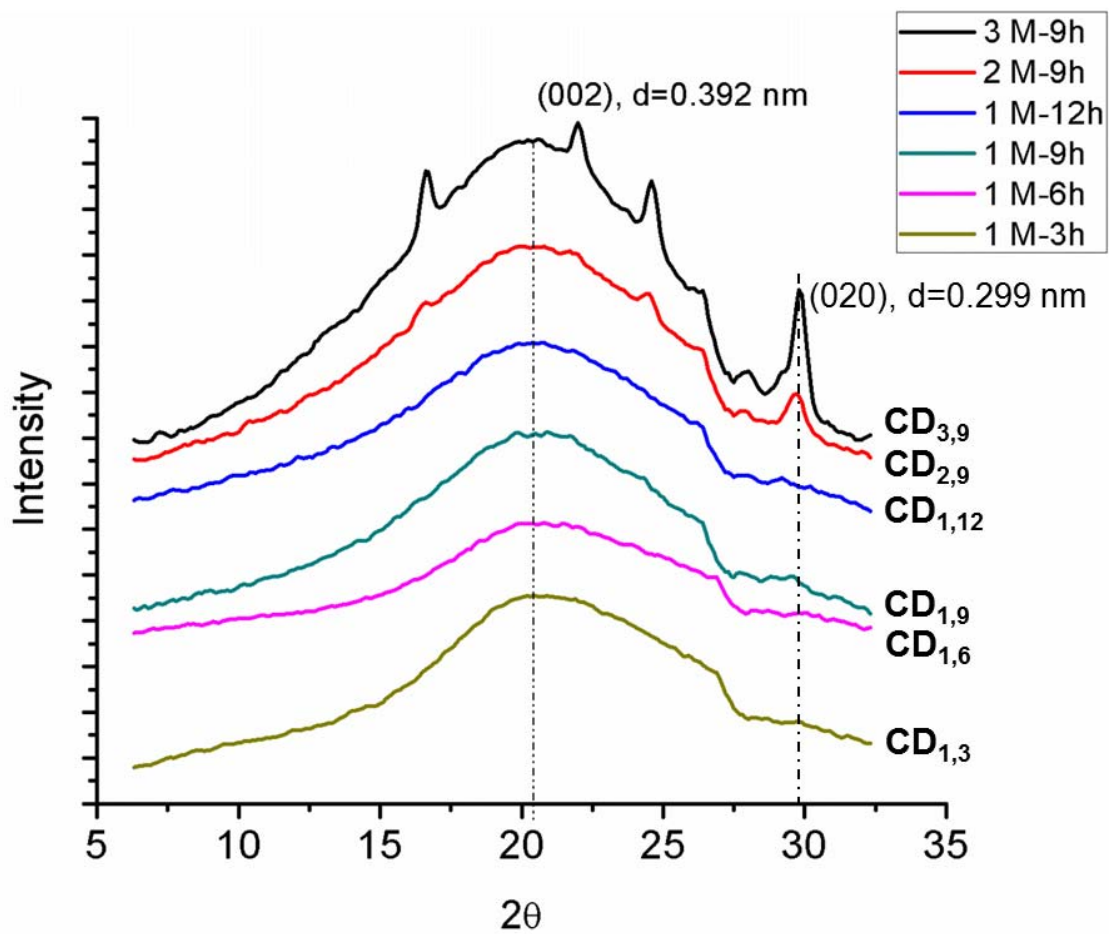


Figure S4. XRD of synthesized CDs.

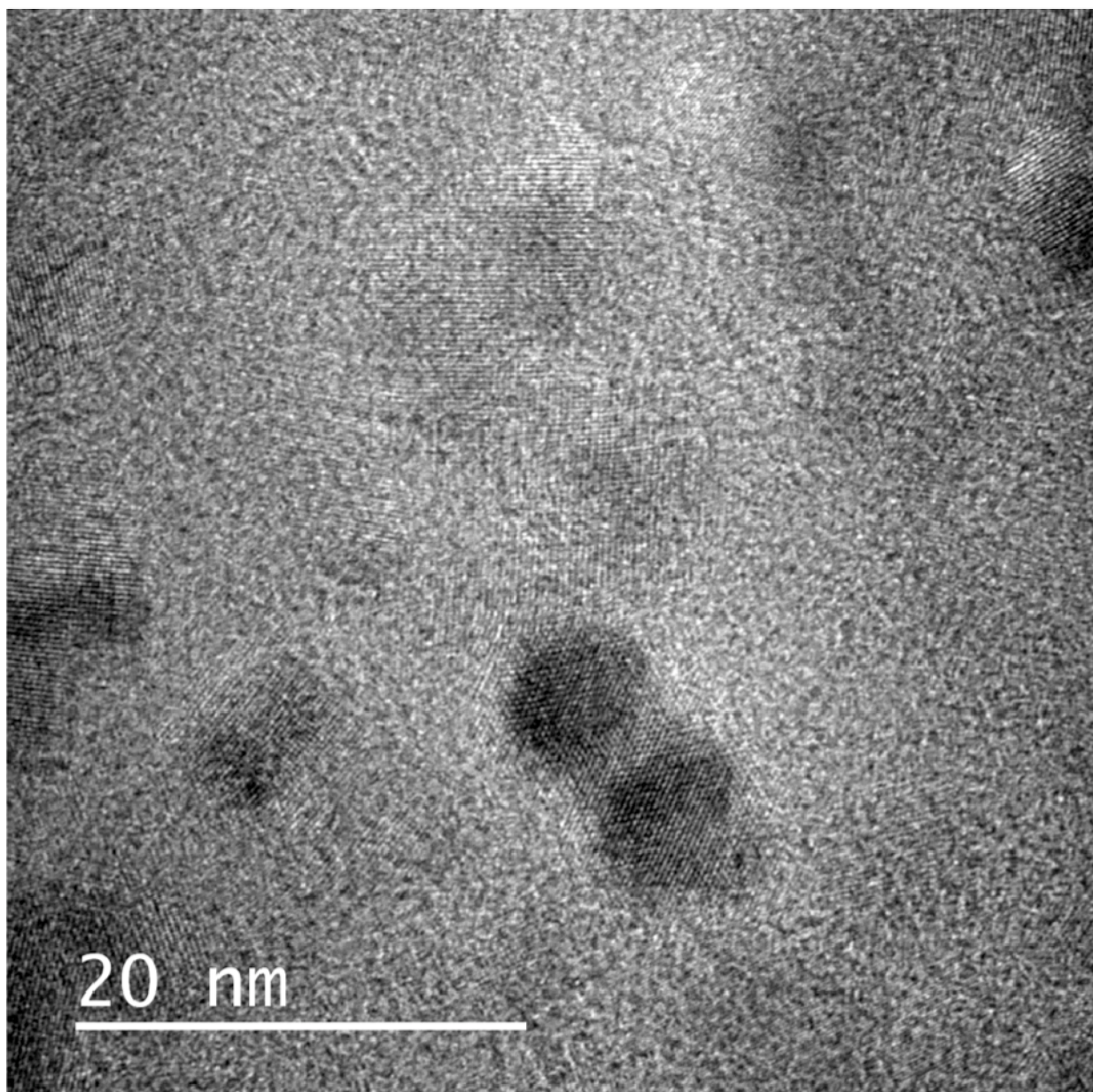


Figure S5. TEM images of CD_{3,9}.

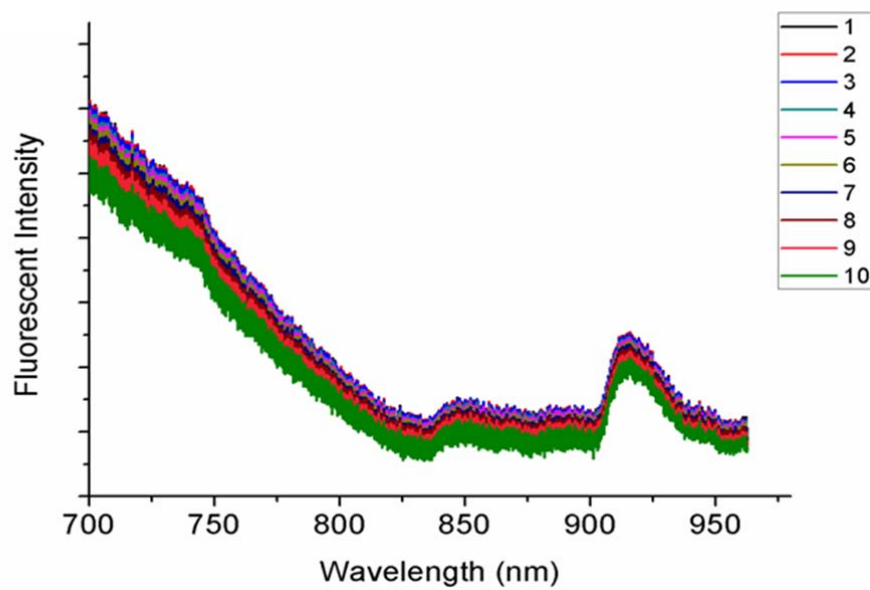


Figure S6. NIR spectra of CD_{3,9} illuminated by a 488-nm laser. Ten times (1-10) of measurement revealed insignificant decay in photostability.

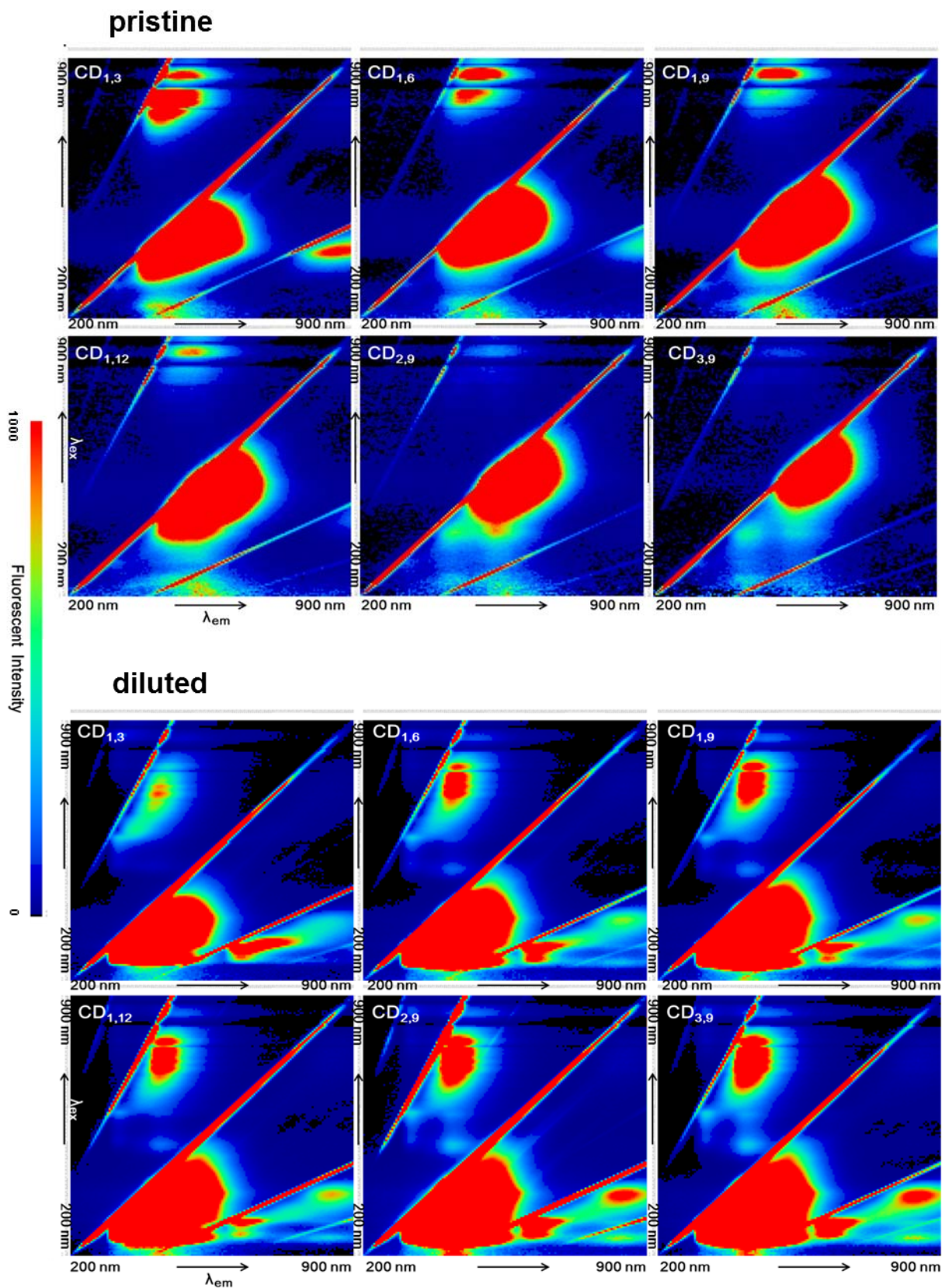


Figure S7. The 3D fluorescence spectra of synthesized CDs. The spectra of pristine CDs (upper six spectra, measured right after synthesis) and that of diluted CDs

(diluted to the absorbance consistent with 0.01 mg mL^{-1} quinine sulfate) were compared. Significant blue-shifts in spectra were observed in diluted CDs with enhanced fluorescence intensity. (x-axis: 200 nm-900 nm of emission wavelengths; y-axis: 200 nm-900 nm of excitation wavelengths; rainbow color gradient: fluorescence intensity). We also observed multiphoton up-conversion fluorescence emission in the spectra of these synthesized CDs.

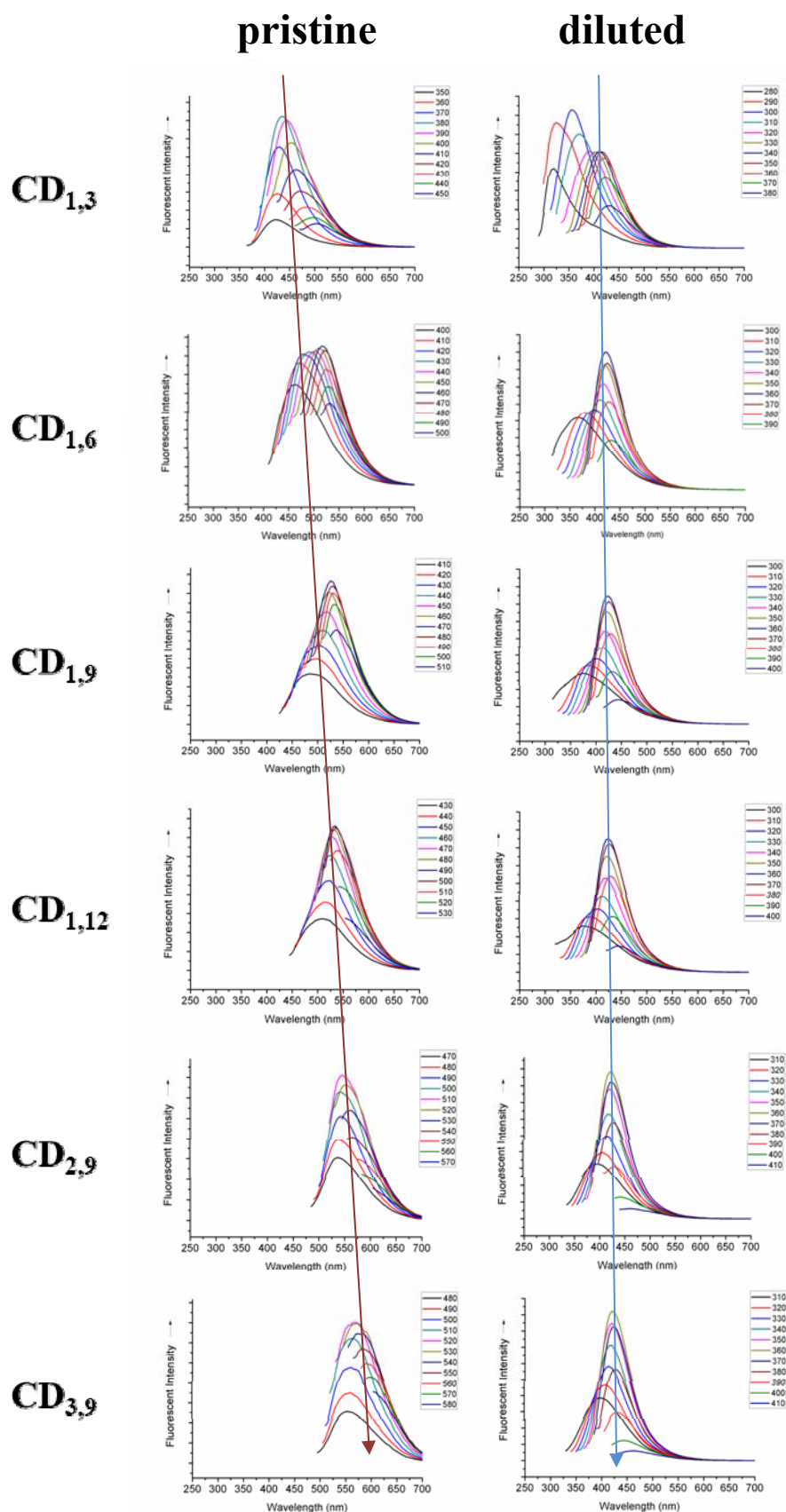


Figure S8. The fluorescence emission spectra of the synthesized CDs excited at specified wavelengths. Whereas remarkable red-shifted spectra were found in

correlation with prolonged reaction time and a high precursor concentration in pristine CD samples (red line arrow), we observed relatively unaltered spectra in the blue region (300–500 nm) (blue line arrow) in all six diluted (normalized using 0.01 mg mL⁻¹ quinine sulfate) CD samples.

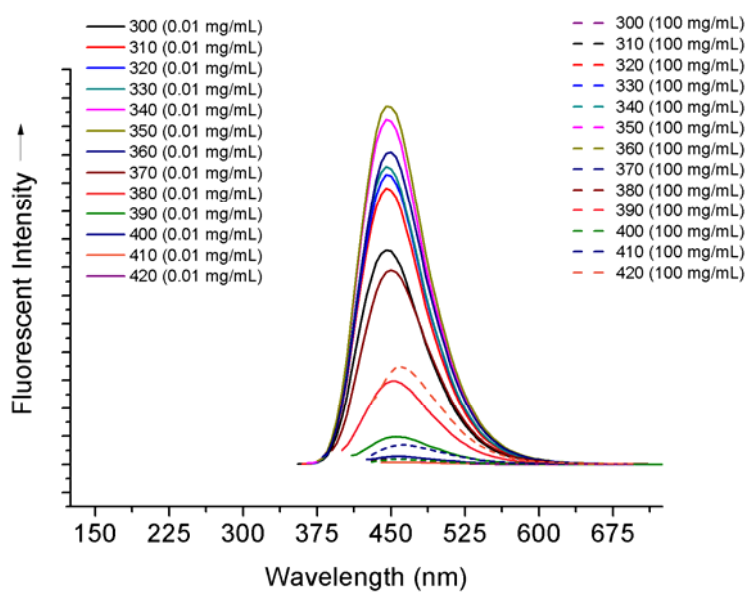


Figure S9. The fluorescence emission spectra of quine sulfate (solid line: low concentration; dash line: high concentration) excited at specified wavelengths.

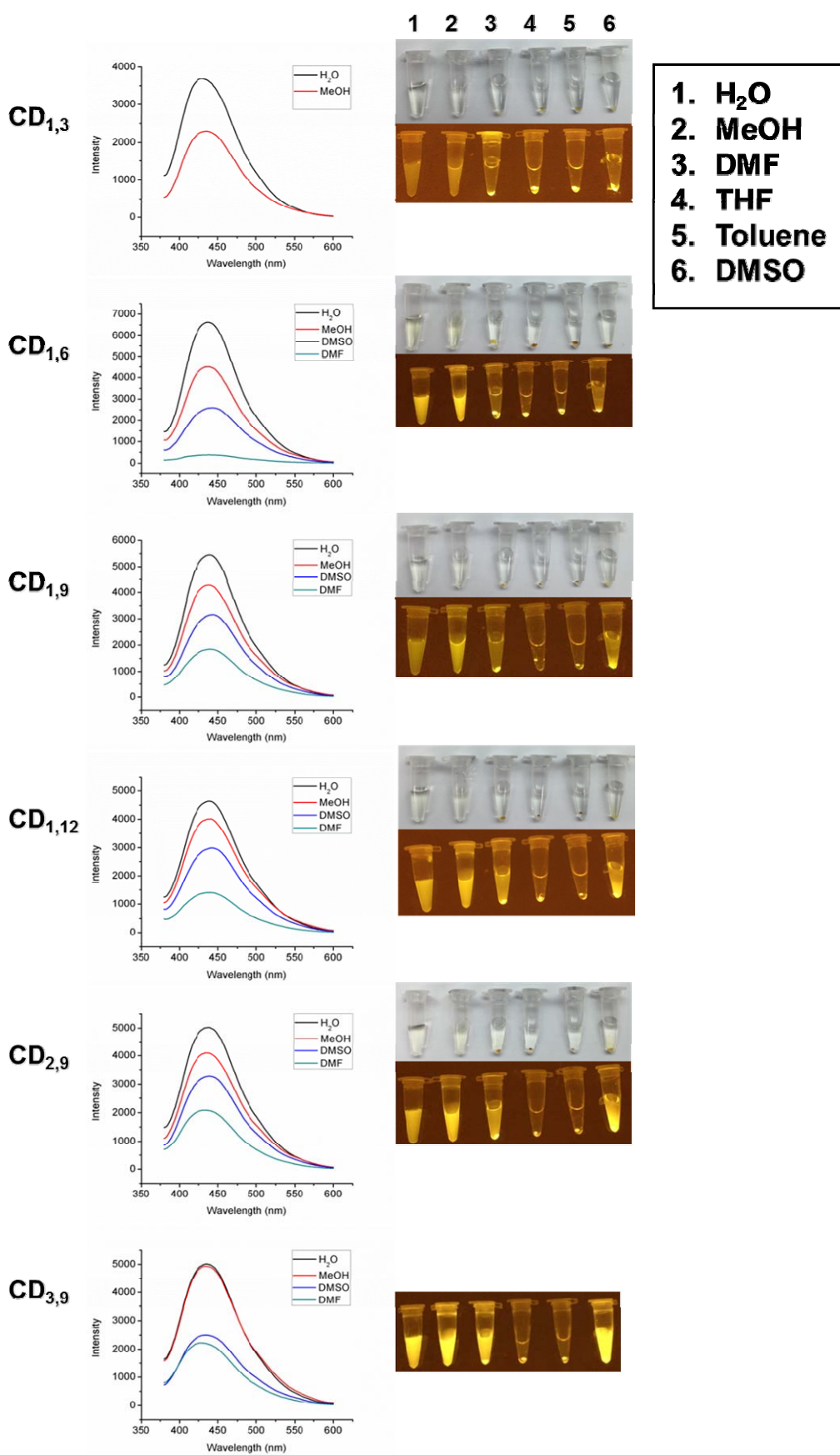


Figure S10. The solubility and the resulting fluorescence in various solvents (excited under a blue light (470 nm) transilluminator)

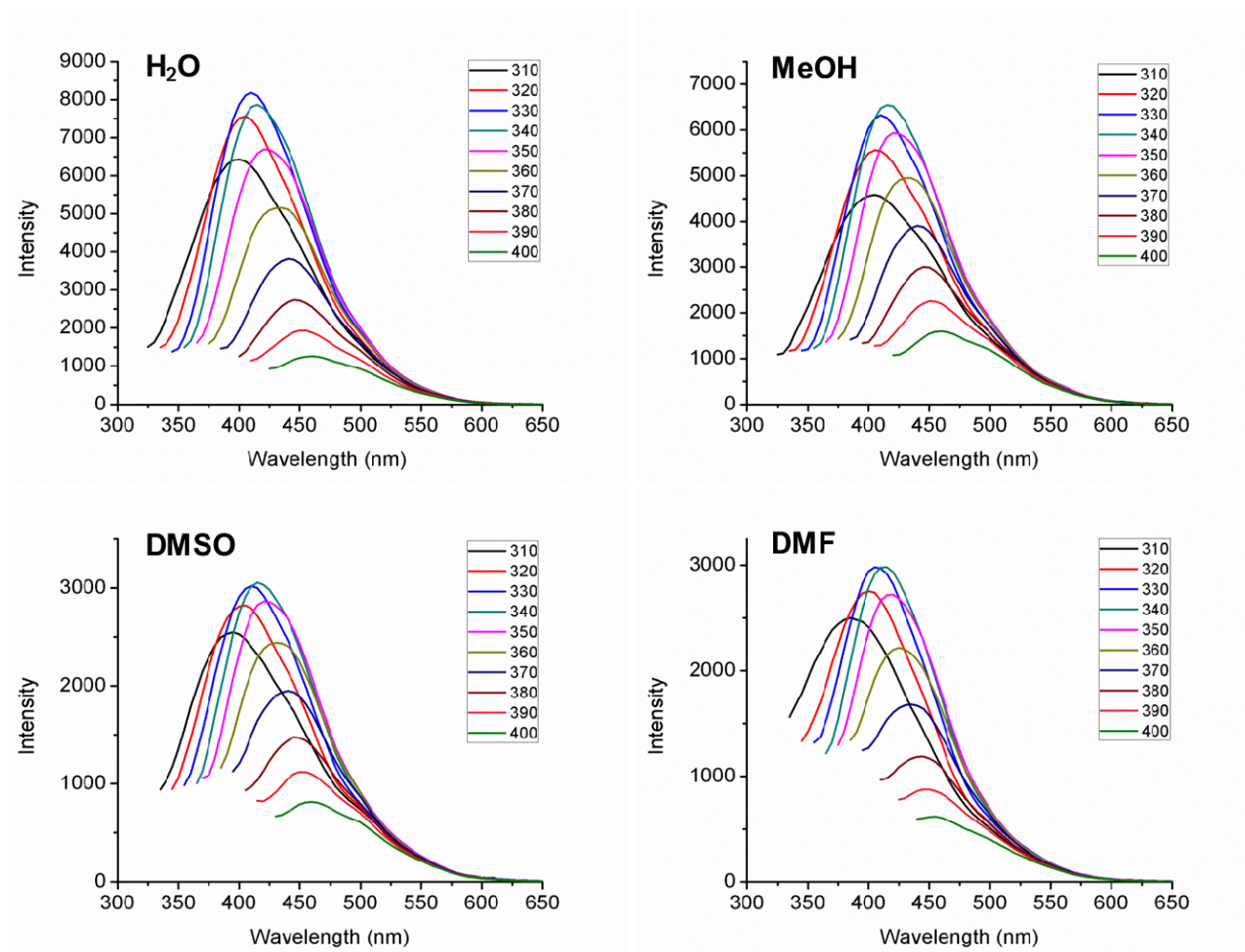


Figure S11. The fluoresce spectra of CD_{3,9} in various solvents. (Due to the insolubility of CD_{3,9} in THF and toluene, their FL spectra were not measured)

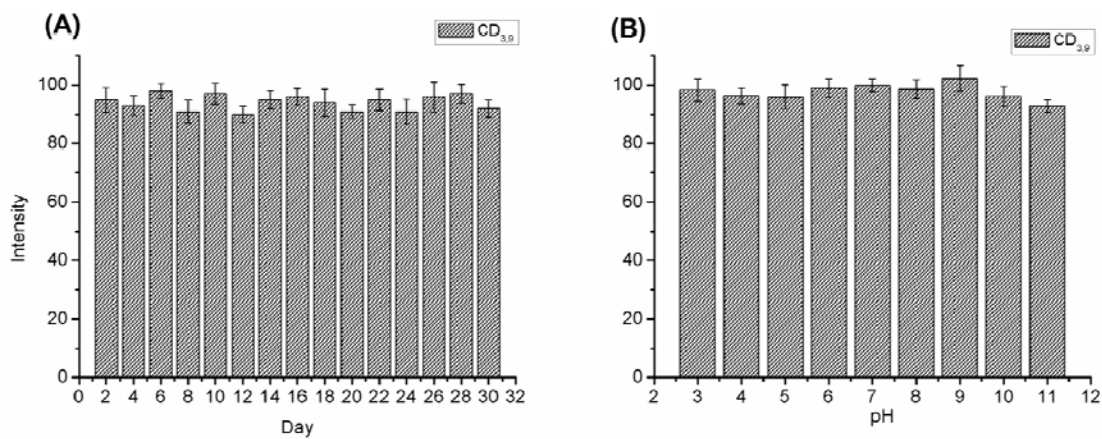


Figure S12. (A) Photo-stability under continuous exposure with a fluorescent lamp (18 W, 380–760 nm) for 1 month. (B) pH-stability in PBS solution.

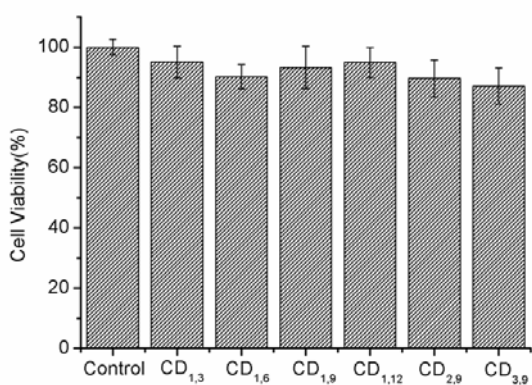


Figure S13. The cytotoxicity of the CDs (1 mg/mL) was determined by MTT assay.

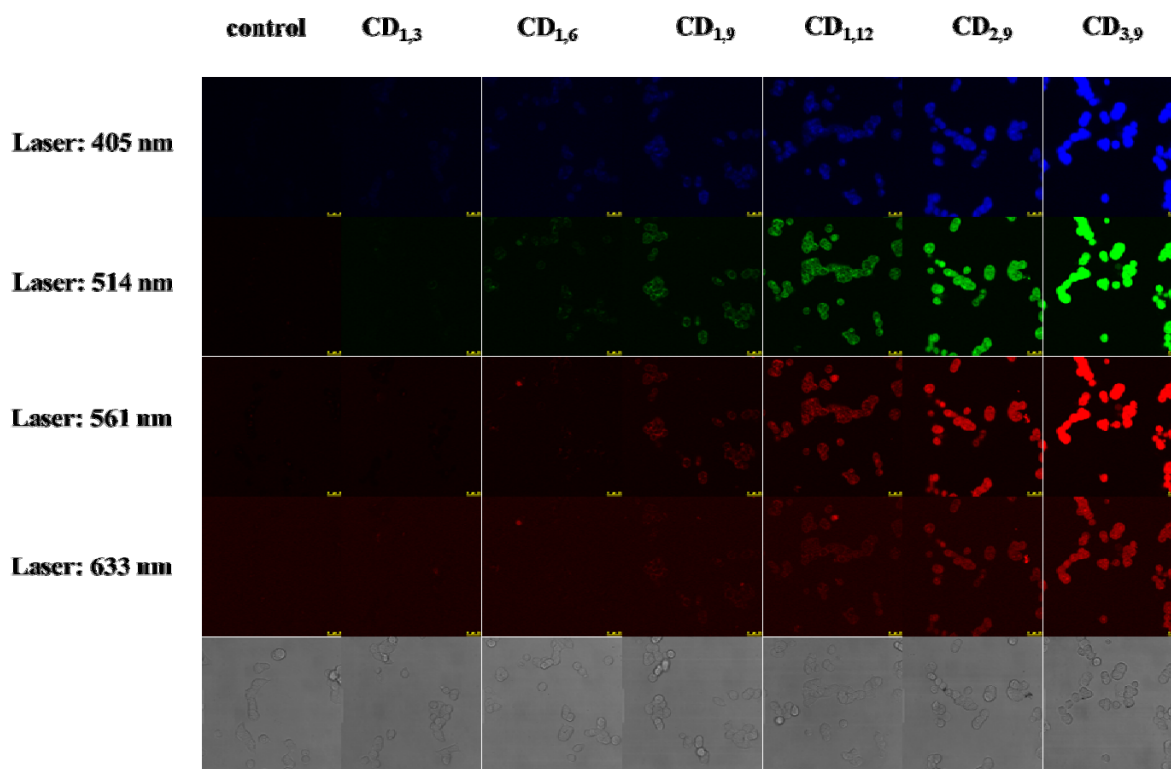


Figure S14. Confocal images of HCT116 cells treated with CD_{1,3}, CD_{1,6}, CD_{1,9}, CD_{1,12}, CD_{2,9}, and CD_{3,9}. Pseudo-colors were employed to represent the emission at various excitation wavelengths. (Control: cell only, without any treatments)

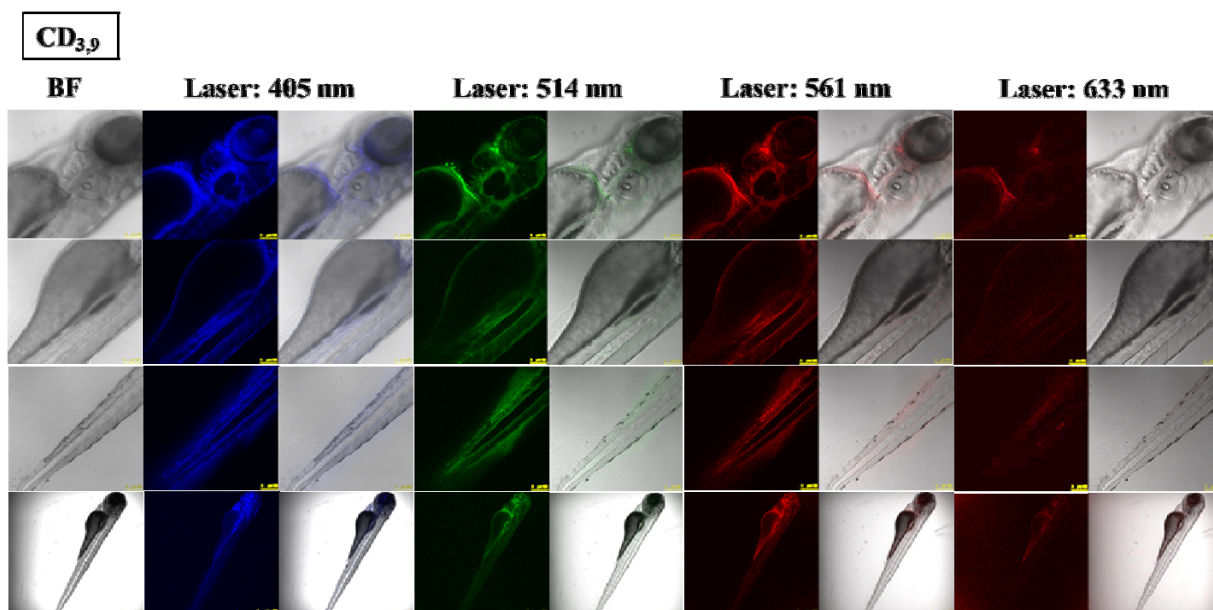
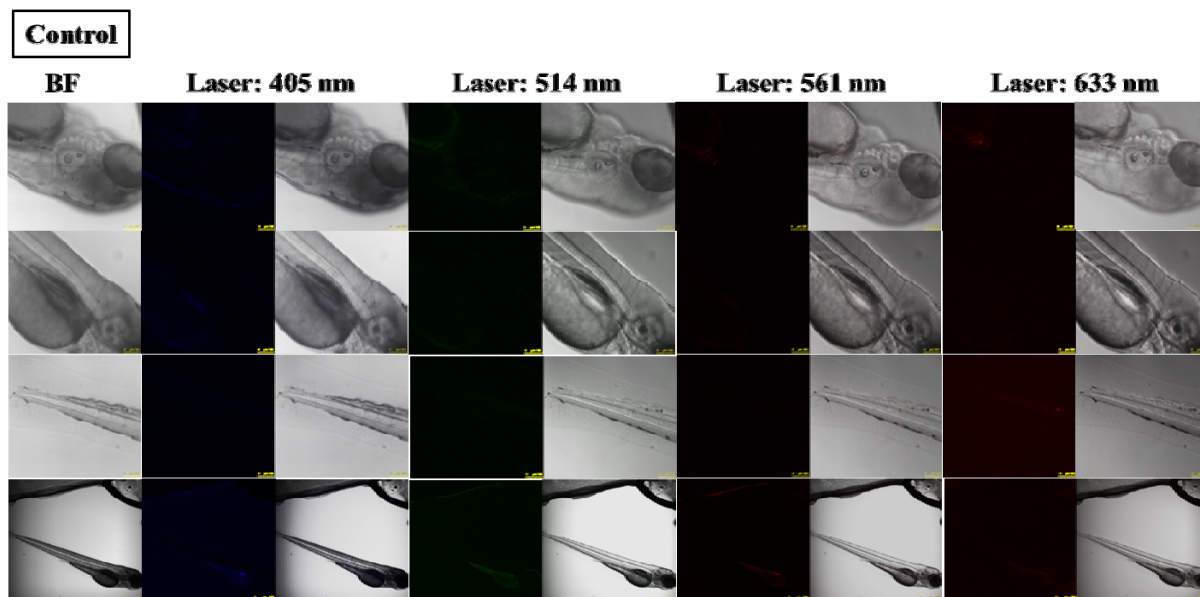


Figure S15. Confocal images of zebrafish containing CD_{3,9} at various excitation wavelengths (405 nm, 514 nm, 561 nm, and 633 nm). Pseudo-colors were employed to represent the emission at various excitation wavelengths. (Control: fish only, without any treatments)